

**Electronic Supplementary Information for:**

**Chemical imaging of Carbide formation and its effect on Alcohol selectivity in Fischer Tropsch Synthesis on Mn-doped Co/TiO<sub>2</sub> pellets**

Danial Farooq<sup>1,2</sup>, Matthew Potter<sup>1,2</sup>, Sebastian Stockenhuber<sup>1,2</sup>, Jay Pritchard<sup>1,2</sup>, Antonios Vamvakarios<sup>3</sup>, Stephen W. T. Price<sup>3</sup>, Jakub Drnec<sup>4</sup>, Ben Ruchte<sup>5</sup>, James Paterson<sup>6</sup>, Mark Peacock<sup>6</sup>, Andrew M. Beale<sup>1,2</sup>

<sup>1</sup>*Department of Chemistry, University College London, 20 Gordon Street, WC1H 0AJ, UK*

<sup>2</sup>*Research Complex at Harwell, Rutherford Appleton Laboratories, Harwell Science and Innovation Campus, Harwell, Didcot, OX11 0FA, UK*

<sup>3</sup>*Finden, Building R71, Harwell Campus, Oxfordshire, OX11 0QX, United Kingdom*

<sup>4</sup>*European Synchrotron Radiation Facility, ID 31 Beamline, BP 220, F-38043 Grenoble Cedex, France*

<sup>5</sup>*IXRF Systems, 10421 Old Manchaca Road, Suite 620, Austin, TX 78748, USA*

<sup>6</sup>*BP, Applied Sciences, Innovation & Engineering, Saltend, Hull, UK*

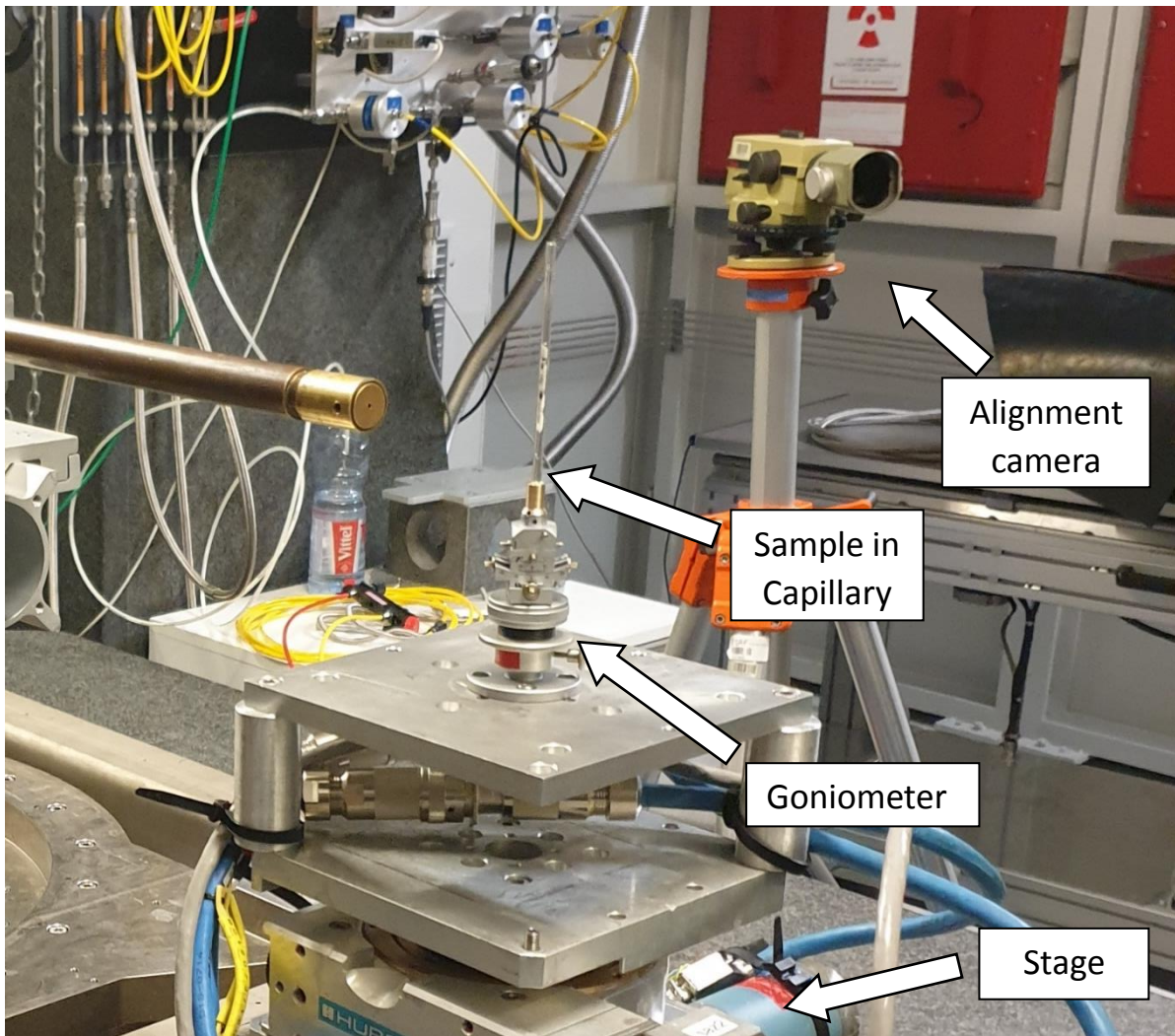


Figure S1 - Experimental set-up at ID31, ESRF, for the XRD-CT and PDF-CT experiments

Table S1 – Crystallographic information of identified phases.

Phase	Space Group	ICSD Code
Co <sub>2</sub> C	P m n n (58)	16895
FCC, Co	F m -3 m (225)	41093
HCP, Co	P 63/m m c (194)	44990
CoO	F m -3 m (225)	9865
Rutile, TiO <sub>2</sub>	P 42/m n m (136)	9161
Anatase, TiO <sub>2</sub>	I 41/ a m d S (141)	9852
MnTiO <sub>3</sub>	R -3 H (148)	60006

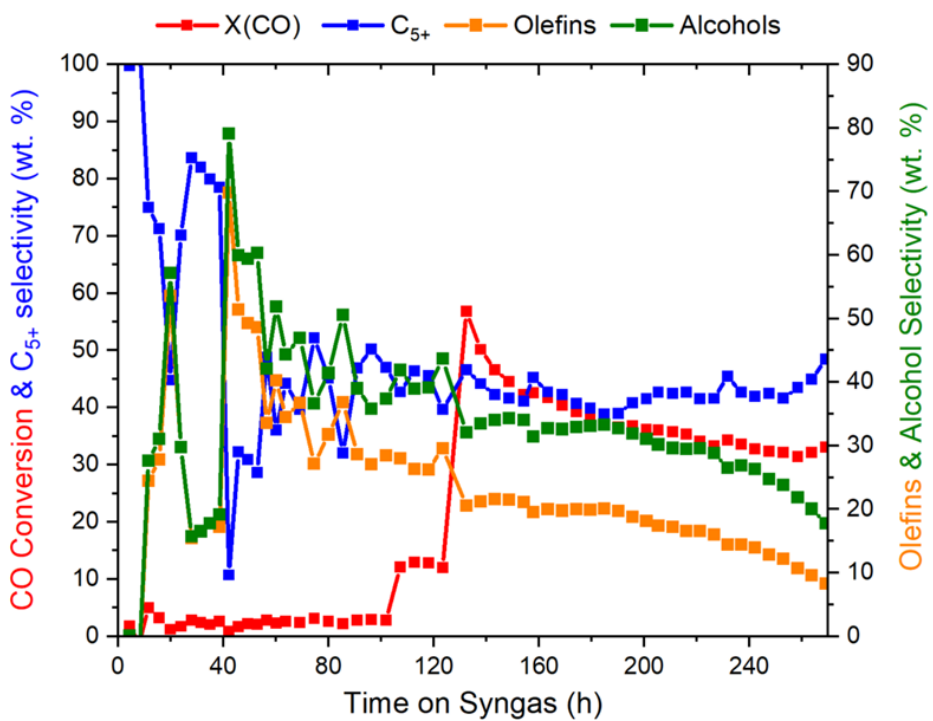


Figure S2 – CO conversion and selectivity to  $C_{5+}$ , alcohols and olefins for the 3 % Mn sample for the reaction time from 0 to 270 h at 30 barg and 210–240 °C. The selectivity and conversion are stable with time on stream after 125 h.

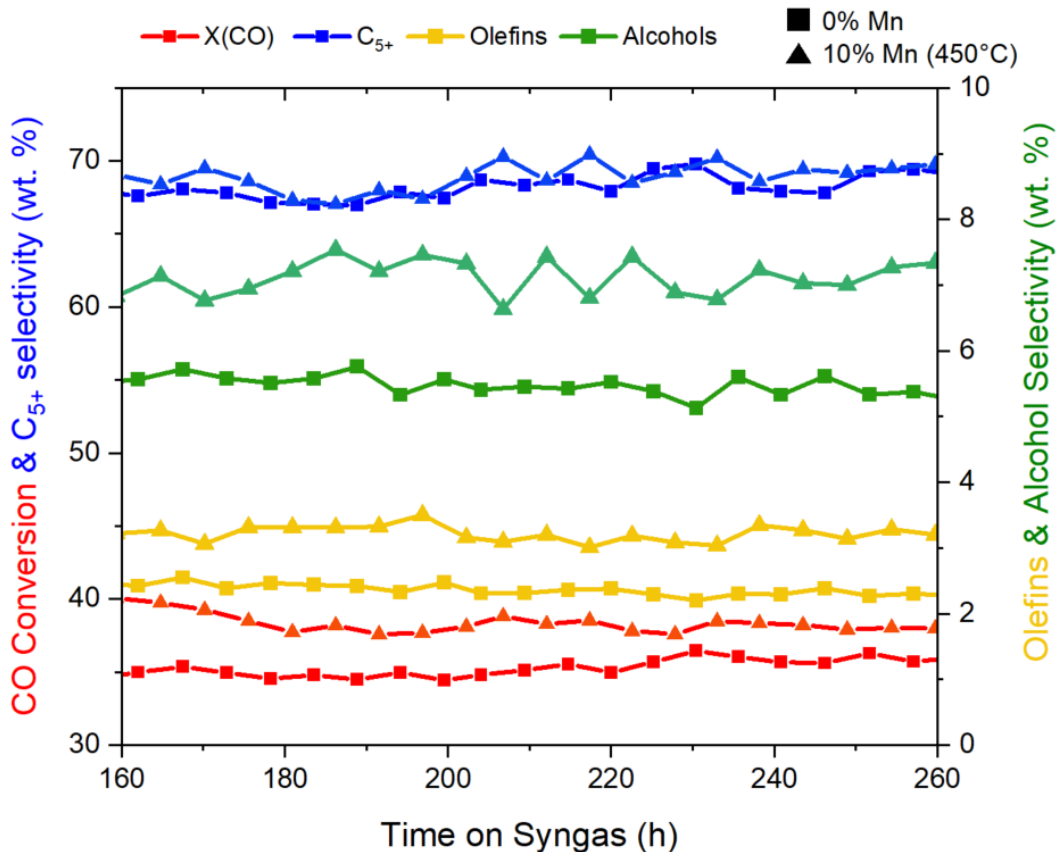


Figure S3 - CO conversion and selectivity to  $C_{5+}$ , alcohols and olefins for the 0 % and 10 % Mn (450 °C) sample for the reaction time from 160 to 300 h at 30 barg and 210–240 °C.

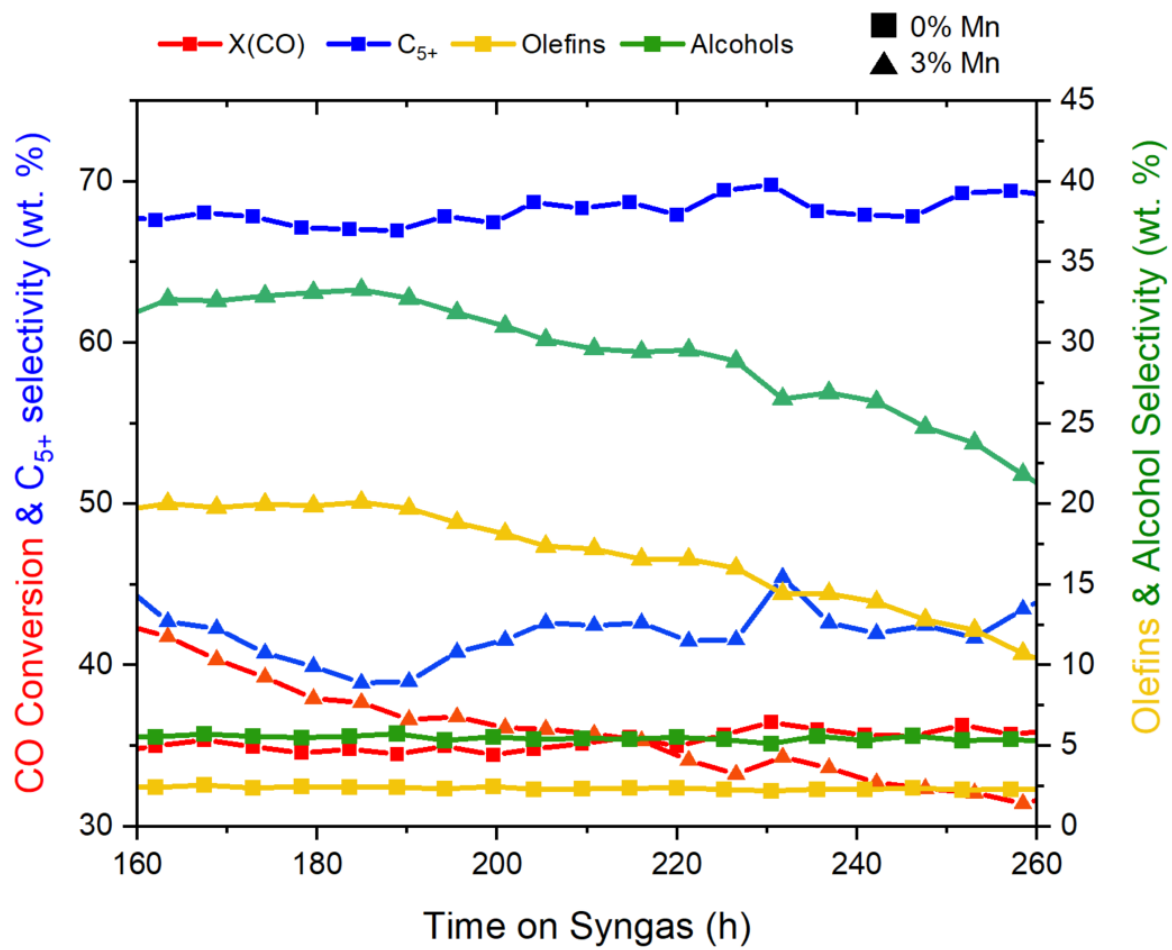


Figure S4 - CO conversion and selectivity to C<sub>5+</sub>, alcohols and olefins for the 0% and 3% Mn sample for the reaction time from 160 to 300 h at 30 barg and 210-240 °C.

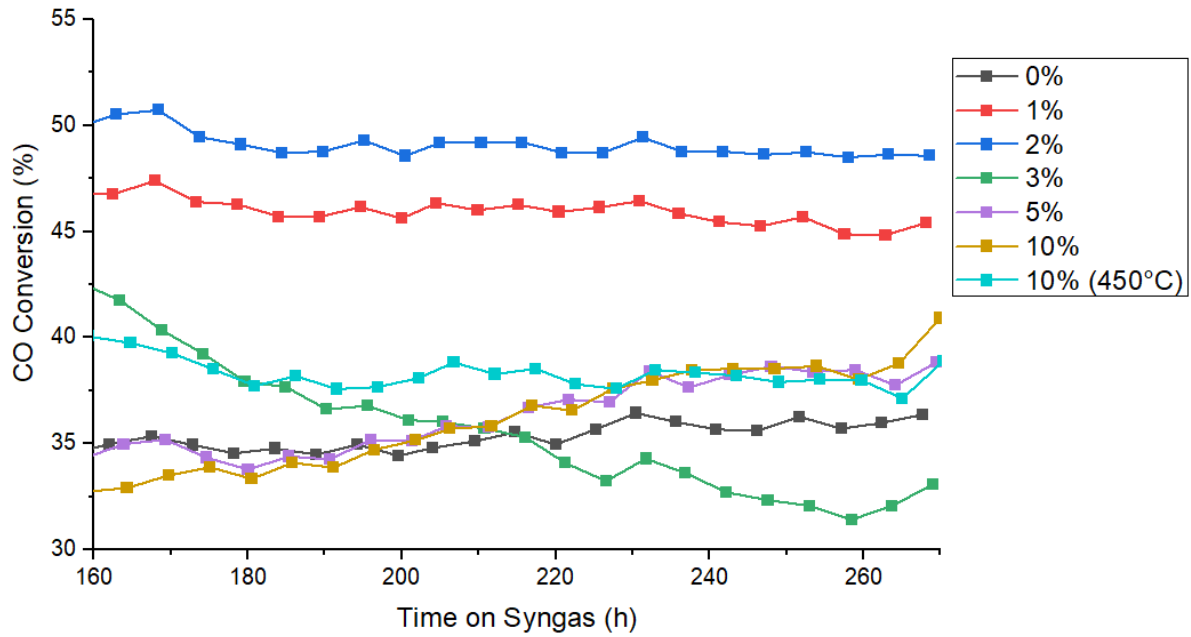


Figure S5 - CO conversion for all the samples tested from 160 – 270 h at 30 barg and 210-240 °C.

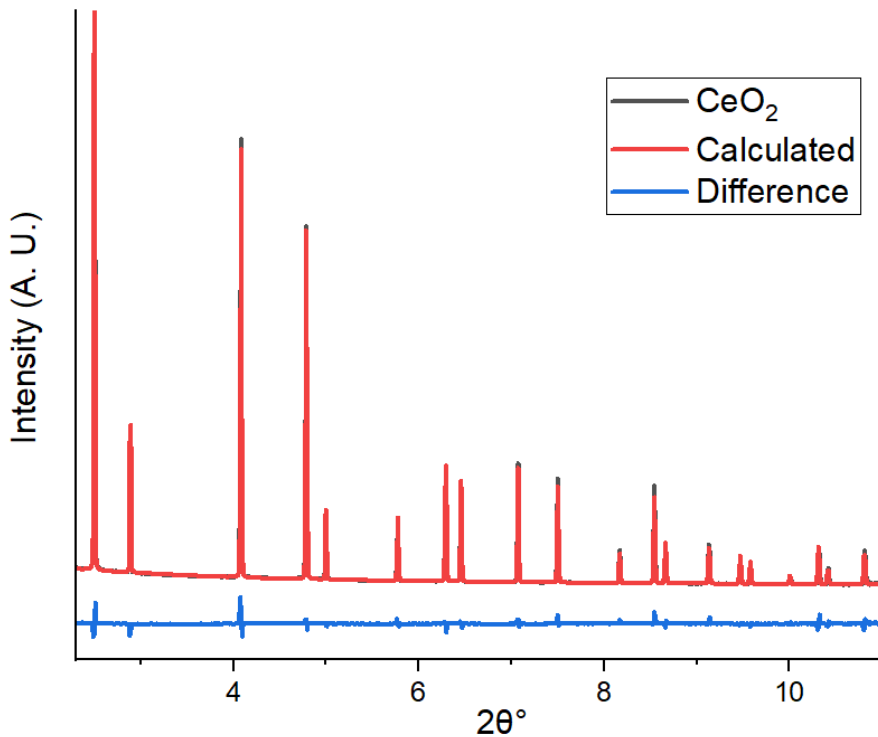


Figure S6 – XRD pattern of the  $\text{CeO}_2$  calibrant, the calculated refined pattern and the difference pattern.

Table S2 - Rietveld Refinement results of the XRD-CT mean patterns illustrating the phase wt. %, CS (crystallite size in nm) and LP (lattice parameters) of the samples extracted after 150 h and 300 h. The  $\text{Co}_2\text{C}$  wt. % increases with Mn loading whilst the  $\text{Co}^0$  metal phases (FCC and HCP) decrease with increasing Mn wt. % beyond 5 %. The 10 % samples reduced at 450 °C resulted in the production of Mn titanates ( $\text{MnTiO}_3$ ).

<sup>a</sup> Reduction at 450 °C

Phase		Mn wt. %							
Time (h)		150	300						
		5 %	0 %	1 %	2 %	3 %	5 %	10 %	10 % <sup>a</sup>
R <sub>wp</sub> (%)		6.4	6.9	6.2	6.2	6.2	6.7	7.9	7.9
$\text{Co}_2\text{C}$	Wt. %	7.5	-	0.6	0.9	3.6	8.9	7.1	-
	CS	7.5	-	-	-	10.6	9.3	11.7	-
	LP (Å)	2.89	-	2.99	2.99	2.89	2.89	2.89	-
		4.45	-	4.61	4.65	4.45	4.45	4.45	-
		4.37	-	4.28	4.26	4.37	4.37	4.37	-
FCC	Wt. %	0.4	3.5	3.3	3.6	1.6	0.1	0.0	2.9
	CS	3.54	10.5	8.1	7.7	5.2	-	-	11.2
	LP (Å)	3.54	3.54	3.54	3.54	3.54	-	-	3.54
HCP	Wt. %	0.2	4.9	4.8	3.8	3.1	0.2	0.7	5.3
	CS	-	2.6	2.2	2.2	7.1	-	9.9	2.9
	LP (Å)	2.51	2.51	2.51	2.52	2.51	2.51	2.50	2.51
		4.10	4.10	4.10	4.06	4.08	4.01	4.21	4.08
CoO	Wt. %	0.9	0.3	0.1	0.2	0.5	1.2	3.1	0.4
	CS	4.0	7.1	3.0	3.7	-	3.3	2.6	5.7

	LP (Å)	4.22	4.28	4.26	4.27	4.24	4.24	4.29	4.28
Rutile	Wt%	10.8	13.5	12.8	11.4	11.4	10.8	8.8	2.6
	CS	25.8	42.6	40.8	39.6	38.2	37.4	28.6	29.1
	LP (Å)	4.60	4.59	4.59	4.59	4.59	4.60	4.60	
		2.96	2.95	2.96	2.96	2.96	2.96	2.96	
Anatase	Wt. %	80.2	77.8	78.4	80.1	79.7	78.9	80.3	65.1
	CS	16.9	21.4	20.7	19.8	19.5	18.9	13.7	15.1
	LP (Å)	3.79	3.79	3.79	3.79	3.79	3.79	3.79	3.79
		9.51	9.50	9.51	9.50	9.50	9.50	9.50	9.50
$\text{MnTiO}_3$	Wt. %							23.7	
	CS							20.8	
	LP (Å)							5.14	
								14.26	

Table S3 –Errors from the Rietveld Refinement results of the XRD-CT mean patterns for the refined phase wt. %, CS (crystallite size in nm) and LP (lattice parameters) of the samples extracted after 150 h and 300 h.

<sup>a</sup> Reduction at 450 °C

Phase		Mn wt. %							
Time (h)		150	300						
		5 %	0 %	1 %	2 %	3 %	5 %	10 %	10 % <sup>a</sup>
Co <sub>2</sub> C	R <sub>wp</sub> (%)	6.4	6.9	6.2	6.2	6.2	6.7	7.9	7.9
	Wt. %	0.696	-	0.078	0.108	0.097	0.139	0.161	-
	CS	0.603	-	-	-	1.36	0.63	1.12	
	LP (Å)	0.001	-	0.007	0.011	0.001	0.001	0.001	-
		0.045	-	0.014	0.022	0.002	0.001	0.002	-
FCC	Wt. %	0.035	0.080	0.074	0.079	0.087	0.047	0.083	0.087
	CS	1.11	1.34	0.73	0.66	1.95	-	-	1.34
	LP (Å)	0.006	0.001	0.001	0.003	-	-	-	0.001
HCP	Wt. %	0.036	0.138	0.128	0.114	0.097	0.052	0.089	0.177
	CS	-	0.27	0.21	0.25	1.25	-	5.7	2.84
	LP (Å)	0.008	0.003	0.003	0.004	0.001	0.003	0.007	0.003
		0.024	0.003	0.010	0.016	0.004	0.008	0.027	0.010
CoO	Wt. %	0.177	0.201	0.126	0.109	0.140	0.200	0.267	0.098
	CS	1.38	4.47	1.95	2.76	-	1.86	1.32	2.90
	LP (Å)	0.023	0.009	0.018	0.047	0.030	0.014	0.007	0.043

Rutile	Wt%	0.775	0.150	0.132	0.133	0.137	0.157	0.221	0.120
CS		5.02	4.07	3.94	4.01	4.02	4.97	5.16	10.4
LP (Å)		4e-4	3e-4	2e-4	3e-4	3e-4	4e-4	8e-4	0.001
		5e-4	3e-4	3e-4	3e-4	3e-4	4e-4	9e-4	0.002
Anatase	Wt %	0.179	0.248	0.210	0.212	0.218	0.254	0.347	0.268
CS		0.56	0.48	0.42	0.39	0.38	0.40	0.31	0.38
LP (Å)		9e-5	1e-4	1e-4	1e-4	1e-4	1e-4	8e-4	2e-4
		4e-4	4e-4	4e-4	4e-4	5e-4	9e-4	9e-4	8e-4
MnTiO <sub>3</sub>	Wt %							0.219	
CS								0.83	
LP (Å)								3e-4	
								0.002	

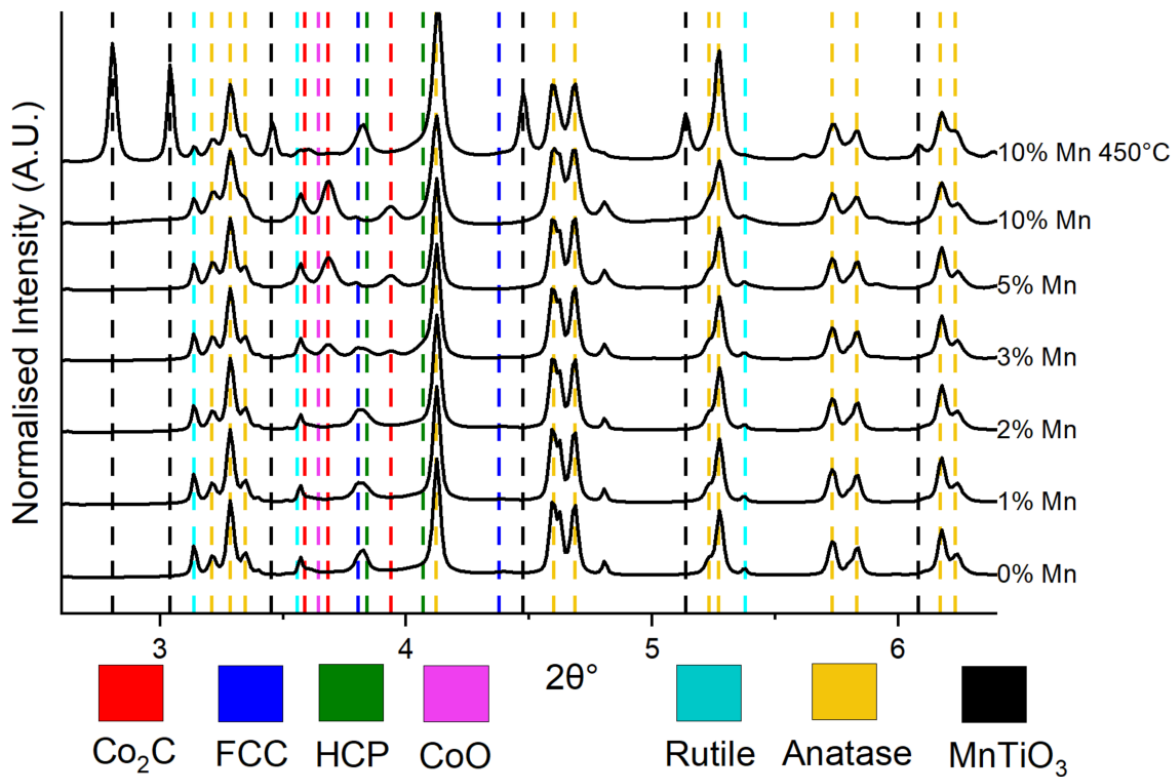


Figure S7 – Full mean XRD pattern of the samples with different Mn loading with indexing lines of all the phases present. FCC and HCP Co phases were present at low Mn loading (0-2 % Mn) and Co<sub>2</sub>C was present at higher Mn loading (3-10 % Mn). A low percentage of Co<sub>x</sub>Mn<sub>1-x</sub>O was present at higher Mn loadings (5-10 %) but its peaks were underneath the Co<sub>2</sub>C peaks. Support phases, anatase and rutile, were present in all samples and MnTiO<sub>3</sub> was present in the sample reduced at 450 °C.

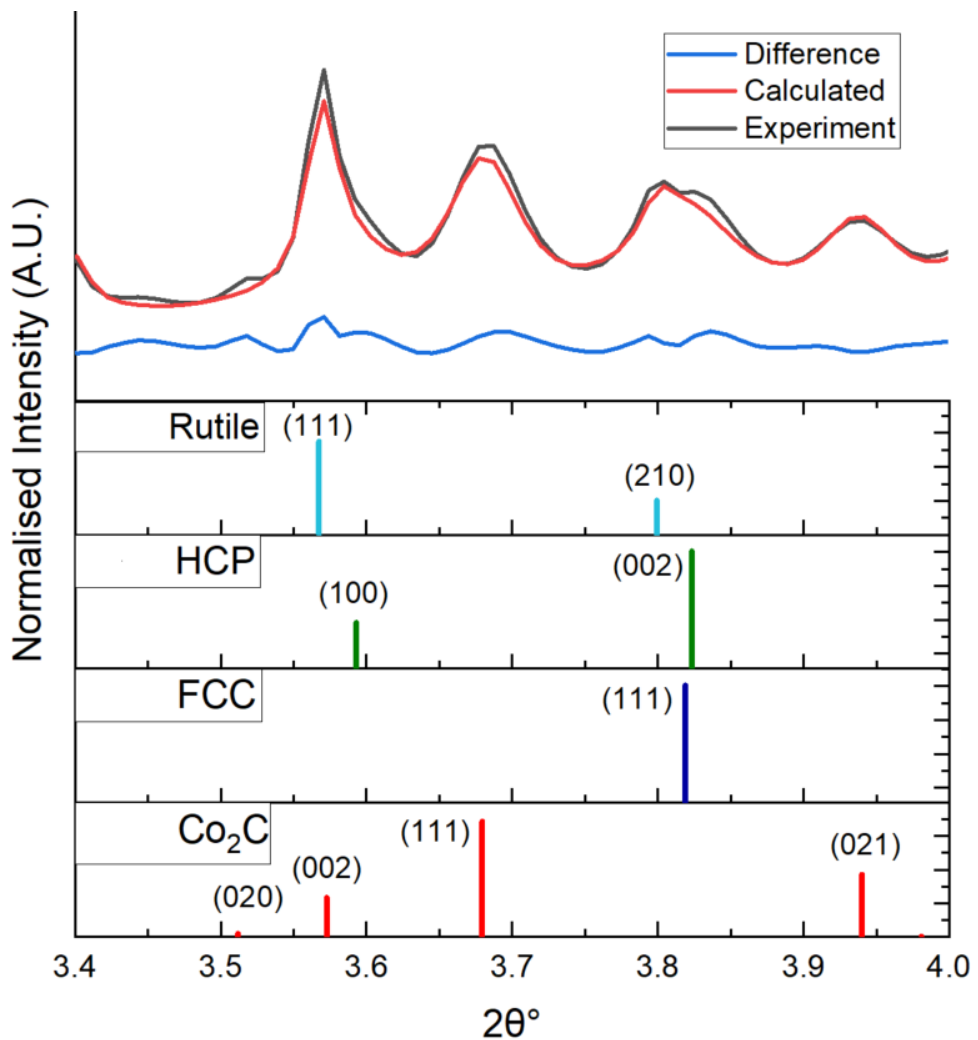


Figure S8 - Mean pattern refinement of the 3 % Mn reacted sample highlighting the  $2\theta^\circ$  region with reflections from the different Co containing phases ( $\text{Co}_2\text{C}$ , FCC and HCP cobalt metal phases respectively). The experimental, refined and difference XRD patterns are displayed as well as the indexing lines for the reference patterns below. The peak shapes are not fitted exactly due to the presence of stacking faults in the FCC/HCP phase, but the  $R_{wp}$  is still low at 6.2 %.

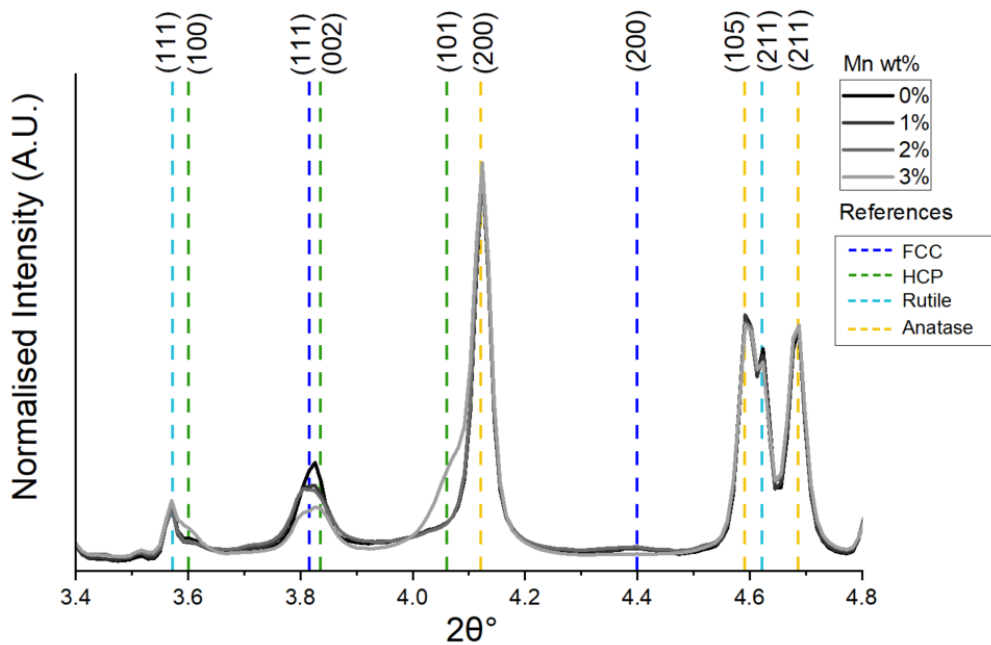


Figure S9 – XRD patterns of the 0-3 % Mn samples from the centre of the extrudates after 300 h of reaction. The 3 % Mn sample has more prominent HCP peaks at  $3.60^\circ$  and  $4.07^\circ$ .

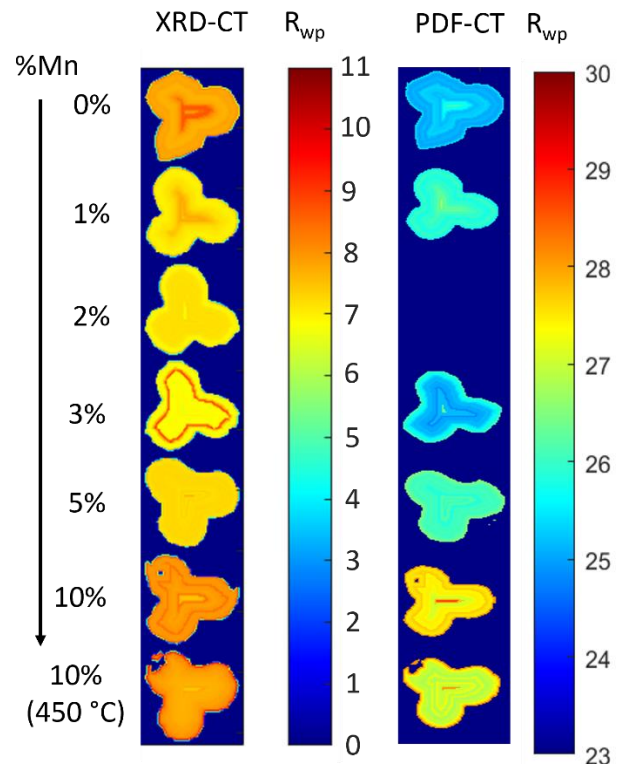
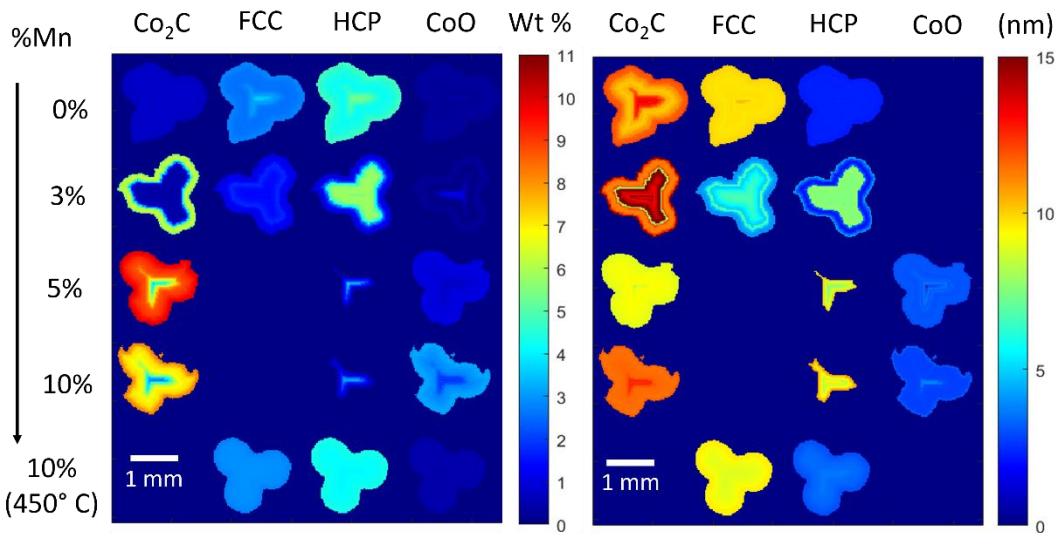
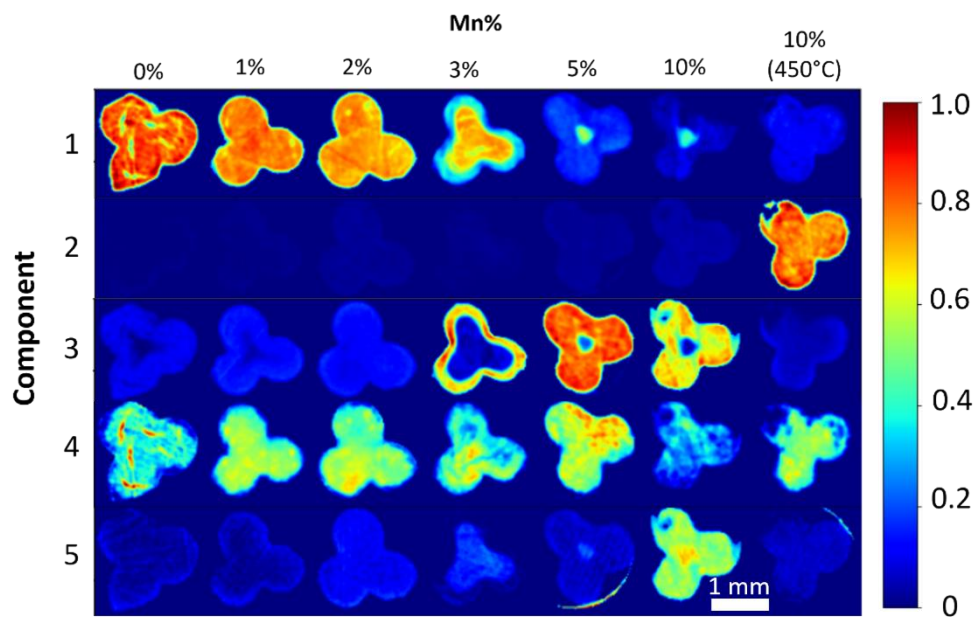


Figure S10 –  $R_{wp}$  maps for the XRD-CT and PDF-CT refinements where the XRD-CT  $R_{wp}$  was between 8 - 10 % indicating a good fit for all the samples. Increasing Mn loading resulted in a larger  $R_{wp}$  indicating increased disorder. The PDF-CT  $R_{wp}$  was between 23 - 28 % which indicates a tolerable fit for PDF data.



*Figure S11 – Reconstructed XRD-CT 2D images of the catalytic pellets (extracted after 300 h) at alternative heights illustrating the refined wt. % percentage (left) and crystallite size (right) of the different phases present. The results at different heights show the same increase in Co<sub>2</sub>C with Mn loading and egg-shell distribution with FCC/HCP in the centre and carbide on the periphery of the pellets.*



*Figure S12 – XRD NMF-generated masks highlighting the spatial intensity variations of the 5 components within the catalytic samples. Component 1 exhibited similarities to the FCC/HCP phases, which tended to concentrate in the core of the catalyst at higher Mn loadings, while Component 3 contained the Co<sub>2</sub>C phase which was found on the catalyst periphery.*

Table S4 – XRD Rietveld refinement results from refining the NMF-generated components. Component 1 was found to contain FCC/HCP phases whilst component 2 contained the MnTiO<sub>3</sub>. Component 3 contained the Co<sub>2</sub>C phase whilst components 4 and 5 had a mixture of different phases. % int. refers to the percentage intensity of each component.

	% int.	Parameter	Co <sub>2</sub> C	FCC	HCP	CoO	Rutile	Anatase	MnTiO <sub>3</sub>	Wax (CH <sub>2</sub> )
1	59	wt. %	-	4.1	3.1	-	10.1	64.9	-	14.7
		CS (nm)	-	5.5	4.9	-	43.4	20.6	-	36.7
		LP (Å)	-	3.54	2.51	-	4.59	3.79	-	2.55
			-	-	4.07	-	2.96	9.50	-	4.96
			-	-	-	-	-	-	-	7.45
2	16	wt. %	-	3.0	3.8	-	2.1	51.6	21.6	17.4
		CS (nm)	-	7.9	3.8	-	-	15.3	20.5	41.4
		LP (Å)	-	3.54	2.5	-	4.59	3.79	5.1	2.55
			-	-	4.1	-	2.96	9.50	14.3	4.96
			-	-	-	-	-	-	-	7.46
3	22	wt. %	7.2	-	-	-	8.6	65.4	-	18.3
		CS (nm)	9.6	-	-	-	37.1	8.6	-	40.6
		LP (Å)	2.89	-	-	-	4.59	3.8	-	2.55
			4.45	-	-	-	2.96	9.5	-	4.96
			4.37	-	-	-	-	-	-	7.44
4	2	wt. %	4.59	1.3	1.0	-	8.8	61.2	-	23.1
		CS (nm)	9.7	6.0	5.7	-	41.2	19.8	-	45.9
		LP (Å)	2.9	3.54	2.50	-	4.59	3.79	-	2.55
			4.4	-	4.08	-	2.96	9.50	-	4.96
			4.4	-	-	-	-	-	-	7.44
5	0.3	wt. %	1.4	-	4.75	2.75	5.67	60.6	-	24.8
		CS (nm)	13.0	-	5.7	2.3	-	14.5	-	34.9
		LP (Å)	2.91	-	2.50	4.28	4.59	3.79	-	2.55
			4.44	-	4.09	4.28	2.96	9.49	-	4.96
			4.36	-	4.75	-	-	-	-	7.44

Table S5 – Errors from the XRD Rietveld refinement of the NMF-generated components.

	% int.	Parameter	Co <sub>2</sub> C	FCC	HCP	CoO	Rutile	Anatase	MnTiO <sub>3</sub>	Wax (CH <sub>2</sub> )
1	59	wt. %	-	0.12	0.14	-	0.18	0.40	-	0.30
		CS (nm)	-	0.70	1.43	-	8.90	1.45	-	3.20
		LP (Å)	-	1e-3	2e-3	-	5e-4	2e-4	-	1e-3
			-	-	7e-3	-	5e-4	7e-4	-	1e-3
			-	-	-	-	-	-	-	2e-3
2	16	wt. %	-	0.10	0.16	-	0.11	0.31	0.23	0.31
		CS (nm)	-	1.33	0.85	-	-	0.96	3.1	19.7
		LP (Å)	-	3e-3	3e-3	-	2e-3	3e-4	6e-4	2e-3
			-	-	0.01	-	3e-3	1e-3	3e-3	2e-3
			-	-	-	-	-	-	-	3e-3
3	22	wt. %	0.15	-	-	-	0.19	0.35	-	0.34
		CS (nm)	1.98	-	-	-	9.16	1.23	-	5.61
		LP (Å)	1e-3	-	-	-	6e-4	2e-4	-	1e-3
			2e-3	-	-	-	6e-4	6e-4	-	1e-3

			2e-3	-	-	-	-	-	-	2e-3
4	2	wt. %	0.13	0.10	0.13	-	0.19	0.36	-	0.36
		CS (nm)	2.10	2.09	3.06	-	10.4	1.51	-	9.7
		LP (Å)	2e-3	4e-3	7e-3	-	5e-4	2e-4	-	8e-4
			3e-3	-	0.02	-	6e-4	6e-4	-	1e-3
			3e-3	-	-	-	-	-	-	1e-3
5	0.3	wt. %	0.19	-	0.25	0.48	0.29	0.66	-	0.64
		CS (nm)	9.02	-	1.36	5.32	-	0.68	-	23.8
		LP (Å)	0.01	-	4e-3	0.12	2e-3	3e-4	-	3e-3
			0.02	-	0.014	0.12	2e-3	1e-3	-	2e-3
			0.03	-	-	-	-	-	-	4e-3

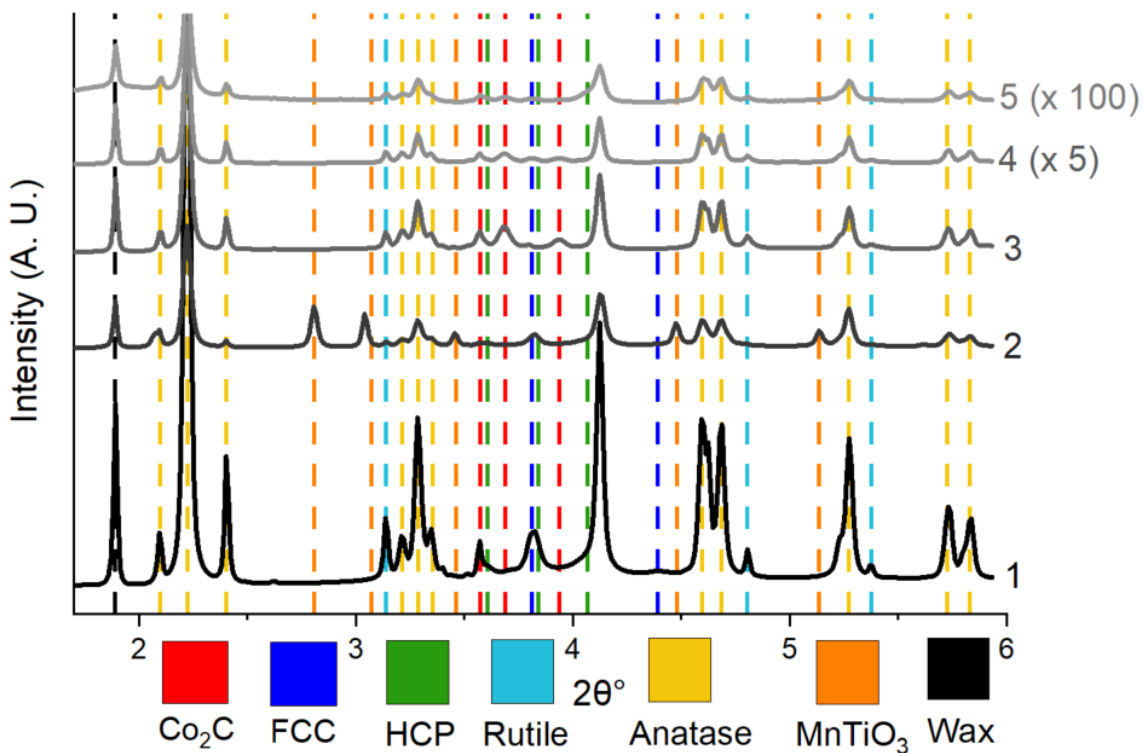


Figure S13 – XRD patterns of the NMF-generated components. All components contained the support phases as the support was homogeneous. Component 1 contained predominantly FCC/HCP Co, component 3 contained Co<sub>2</sub>C and component 2 contained MnTiO<sub>3</sub>. Components 4 and 5 were multiplied by 5 and 100, respectively, for visibility.

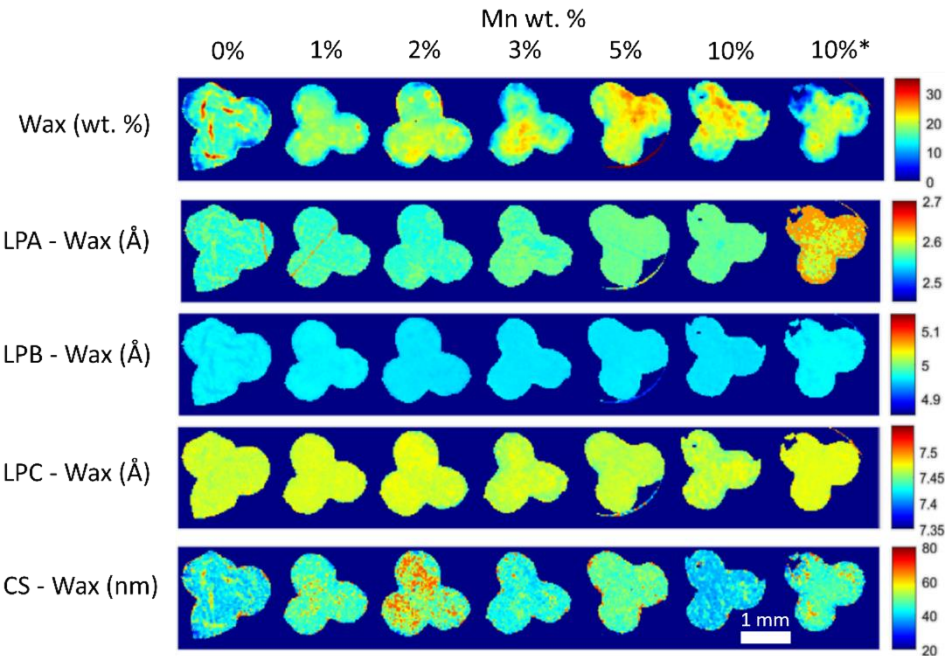


Figure S14 - XRD-CT maps of the refined parameters of the wax content (wt. %), lattice parameters (LPA, LPB and LPC), and crystallite size (CS). \*Reduced at 450 °C during preparation.

Table S6 – Real-space Refinement results of the PDF-CT mean patterns illustrating the phase wt. %, CS (crystallite size) and LP (lattice parameters). The results correlate well with the XRD refinement. Co<sub>2</sub>C wt. % increases with Mn loading whilst the Co<sup>0</sup> metal phases (FCC and HCP) decrease with increasing Mn wt. % beyond 5 %.

<sup>a</sup> Reduction at 450° C

Phase	Parameter	Mn wt. %					
		0 %	1 %	3 %	5 %	10 %	10 % <sup>a</sup>
	R <sub>wp</sub> (%)	21.6	21.5	21.1	22.1	23.5	25.8
Co <sub>2</sub> C	Wt. %	1.1	1.1	3.7	9.1	9.5	1.3
	CS (nm)	-	-	-	15.6	12.0	-
	LP (Å)	2.87	2.87	2.88	2.88	2.88	2.87
FCC		4.41	4.42	4.43	4.43	4.43	4.42
		4.39	4.39	4.37	4.37	4.37	4.39
	Wt. %	5.7	5.4	1.7	-	0.0	5.0
HCP	CS (nm)	4.0	3.7	4.1	-	-	8.5
	LP (Å)	3.53	3.54	3.54	-	-	3.53
	Wt. %	5.0	4.8	5.4	0.3	0.2	2.2
CoO	CS (nm)	3.9	3.6	4.2	-	-	5.6
	LP (Å)	2.49	2.50	2.50	2.58	2.60	2.73
	Wt. %	1.1	1.1	1.0	1.1	5.2	1.7

	CS (nm)	2.1	1.9	1.6	1.1	1.0	2.6
	LP (Å)	4.25	4.26	4.26	4.26	4.34	4.29
Rutile	Wt. %	15.8	15.2	13.9	12.8	11.6	5.2
	CS (nm)	4.3	4.4	4.4	4.6	4.2	4.6
	LP (Å)	4.59	4.59	4.59	4.59	4.60	4.62
Anatase		2.95	2.95	2.95	2.95	2.94	2.91
	Wt. %	71.1	72.1	74.0	76.2	73.2	59.3
	CS (nm)	5.1	5.1	5.0	5.0	4.5	4.6
	LP (Å)	3.78	3.78	3.78	3.78	3.78	3.78
$\text{MnTiO}_3$	Wt. %					25.8	
	CS (nm)					9.30	
	LP (Å)					5.12	
						14.23	

Table S7 – Errors from the Real-space Refinement results of the PDF-CT mean patterns for the phase wt. %, CS (crystallite size) and LP (lattice parameters).

<sup>a</sup> Reduction at 450° C

Phase	Parameter	Mn wt. %					
		0 %	1 %	3 %	5 %	10 %	10 % <sup>a</sup>
$\text{Co}_2\text{C}$	$R_{wp}(\%)$	21.6	21.5	21.1	22.1	23.5	25.8
	Wt. %	0.204	0.205	0.214	0.281	0.252	0.103
	CS (nm)	-	-	-	3.96	0.46	-
	LP (Å)	0.006	0.006	0.002	0.001	0.001	0.005
		0.009	0.010	0.003	0.002	0.001	0.008
		0.010	0.011	0.003	0.002	0.001	0.009
FCC	Wt. %	0.157	0.166	0.160	0.17	0.16	0.19
	CS (nm)	0.15	0.14	0.51	0.01	-	0.42
	LP (Å)	6e-4	7e-4	0.003	-	0.74	7e-4
HCP	Wt. %	0.338	0.343	0.314	0.192	0.178	0.239
	CS (nm)	0.30	0.33	0.41	-	-	0.084
	LP (Å)	0.002	0.003	0.002	0.004	0.006	0.001
CoO		0.007	0.008	0.006	0.014	0.020	0.004
	Wt. %	0.221	0.012	0.200	0.185	0.515	0.316



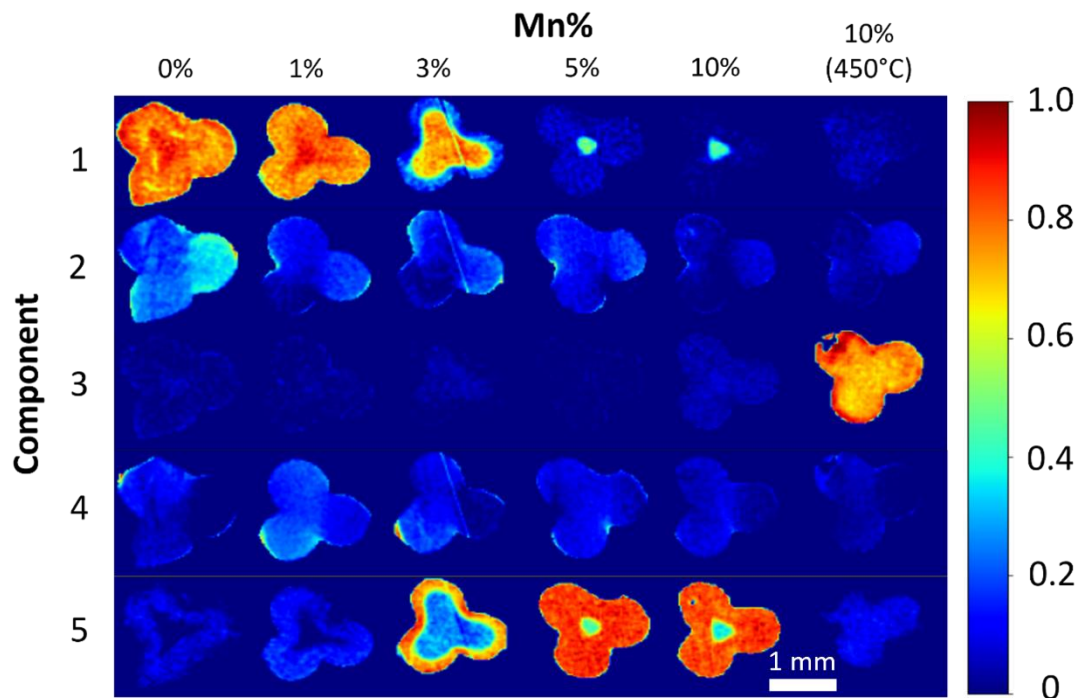


Figure S15 – PDF-CT NMF-generated masks highlighting the spatial intensity variations of the 5 components within the catalytic samples. Component 1 exhibited similarities to the FCC/HCP phases, which tended to concentrate in the core of the catalyst at higher Mn loadings, while Component 5 contained the Co<sub>2</sub>C phase which was found on the catalyst periphery.

Table S8 – PDF Real-space refinement results from refining the NMF-generated components. Component 1 was found to contain FCC/HCP phases whilst component 3 contained the MnTiO<sub>3</sub>. Component 5 contained the Co<sub>2</sub>C phase whilst components 2 and 4 had a mixture of different phases but had low intensity. % int. refers to the percentage intensity of each component.

	%. int	Parameter	Co <sub>2</sub> C	FCC	HCP	CoO	Rutile	Anatase	MnTiO <sub>3</sub>
<b>1</b>	43	wt. %	-	5.4	5.7	4.7	14.5	69.7	-
		CS (nm)	-	3.4	4.1	0.8	4.5	5.0	-
		LP (Å)	-	3.53	2.49	4.44	4.59	3.78	-
			-	4.10	-	2.95	9.47	-	-
			-	-	-	-	-	-	-
<b>2</b>	0.1	wt. %	-	5.0	4.1	4.4	13.1	67.4	-
		CS (nm)	-	5.3	3.8	0.7	4.9	5.7	-
		LP (Å)	-	3.53	2.48	4.42	4.57	3.77	-
			-	4.10	-	2.4	9.44	-	-
			-	-	-	-	-	-	-
<b>3</b>	15	wt. %	-	6.0	6.6	3.0	5.0	52.1	27.3
		CS (nm)	-	3.5	3.7	0.9	4.5	4.8	6.8
		LP (Å)	-	3.53	2.50	4.41	4.60	3.78	5.1
			-	4.10	-	2.93	9.47	14.2	-
			-	-	-	-	-	-	-
<b>4</b>	0.2	wt. %	5.5	1.6	3.4	7.7	11.0	70.8	-
		CS (nm)	12.5	8.8	5.8	0.7	3.7	6.2	-
		LP (Å)	2.90	3.55	2.58	4.5	4.6	3.79	-
			4.42	-	4.09	-	2.96	9.50	-

			4.40	-	-	-	-	-	-
5	42	wt. %	10.6	-	-	5.1	12.1	72.1	-
		CS (nm)	7.8	-	-	0.8	4.5	4.8	-
		LP (Å)	2.88	-	-	4.41	4.59	3.78	-
			4.42	-	-	-	2.94	9.47	-
			4.37	-	-	-	-	-	-

Table S9 – Errors from the PDF Real-space refinement results of the NMF-generated components.

	%. int	Parameter	Co <sub>2</sub> C	FCC	HCP	CoO	Rutile	Anatase	MnTiO <sub>3</sub>
1	43	wt. %	-	0.12	0.24	0.37	0.22	0.42	-
		CS (nm)	-	0.09	0.28	0.68	0.12	0.03	-
		LP (Å)	-	5e-4	2e-3	7e-3	6e-4	1e-4	-
			-	-	5e-3	-	8e-4	5e-4	-
			-	-	-	-	-	-	-
2	0.1	wt. %	-	0.14	0.34	0.60	0.30	0.61	-
		CS (nm)	-	0.23	0.50	0.12	0.20	0.05	-
		LP (Å)	-	7e-4	3e-3	0.01	1e-3	2e-4	-
			-	-	0.01	-	1e-3	7e-4	-
			-	-	-	-	-	-	-
3	15	wt. %	-	0.08	0.18	0.23	0.15	0.26	0.31
		CS (nm)	-	0.73	0.20	0.09	0.27	0.03	0.16
		LP (Å)	-	4e-4	1e-3	9e-3	2e-3	2e-4	5e-4
			-	-	4e-3	-	2e-3	6e-4	2e-3
			-	-	-	-	-	-	-
4	0.2	wt. %	0.50	0.12	0.31	0.67	0.39	0.71	-
		CS (nm)	3.0	2.0	1.25	0.08	0.22	0.66	-
		LP (Å)	2e-3	3e-3	5e-3	0.01	2e-3	2e-3	-
			3e-3	-	0.01	-	2e-3	8e-3	-
			4e-3	-	-	-	-	-	-
5	42	wt. %	0.31	-	-	0.33	0.21	0.37	-
		CS (nm)	0.45	-	-	0.06	0.14	0.03	-
		LP (Å)	7e-3	-	-	7e-3	8e-3	1e-4	-
			1e-3	-	-	-	1e-3	5e-4	-
			1e-3	-	-	-	-	-	-

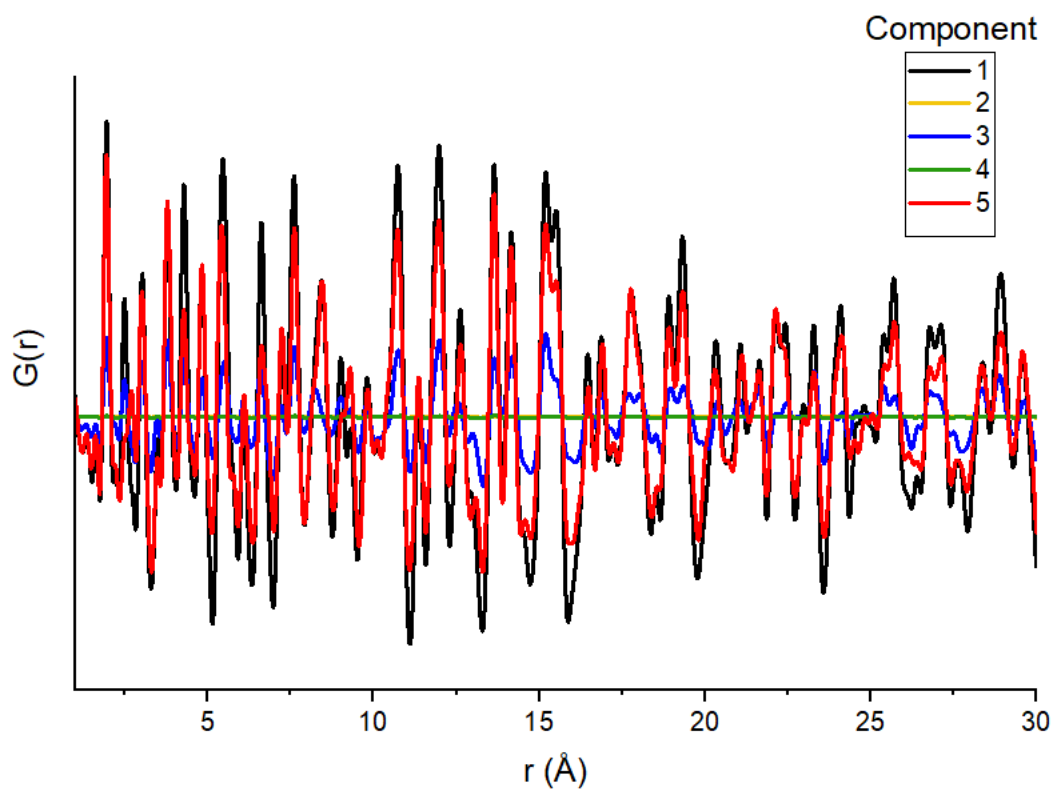


Figure S16 – PDF of the NMF-generated components. All components contained the support phases as the support was homogeneous. Component 1 contained predominantly FCC/HCP Co, component 5 contained  $\text{Co}_2\text{C}$  and component 3 contained  $\text{MnTiO}_3$ .

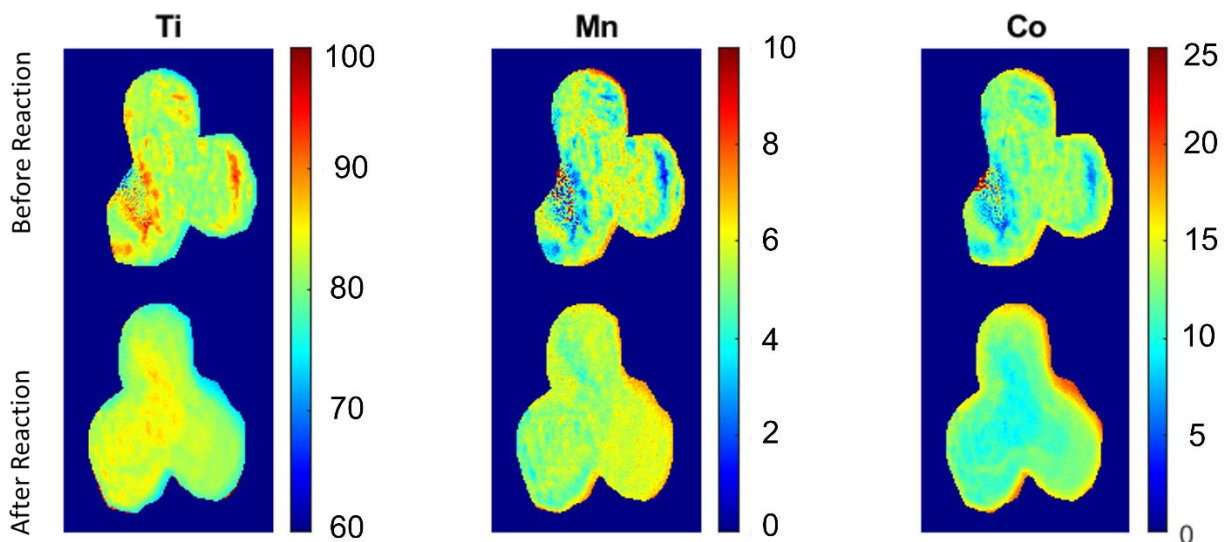


Figure S17 –  $\mu$ -XRF images (intensity (%)) of the cross-sections (right) of the 3 wt. % Mn samples extracted before and after reaction for 300 h. The Mn and Co are found to be co-located.

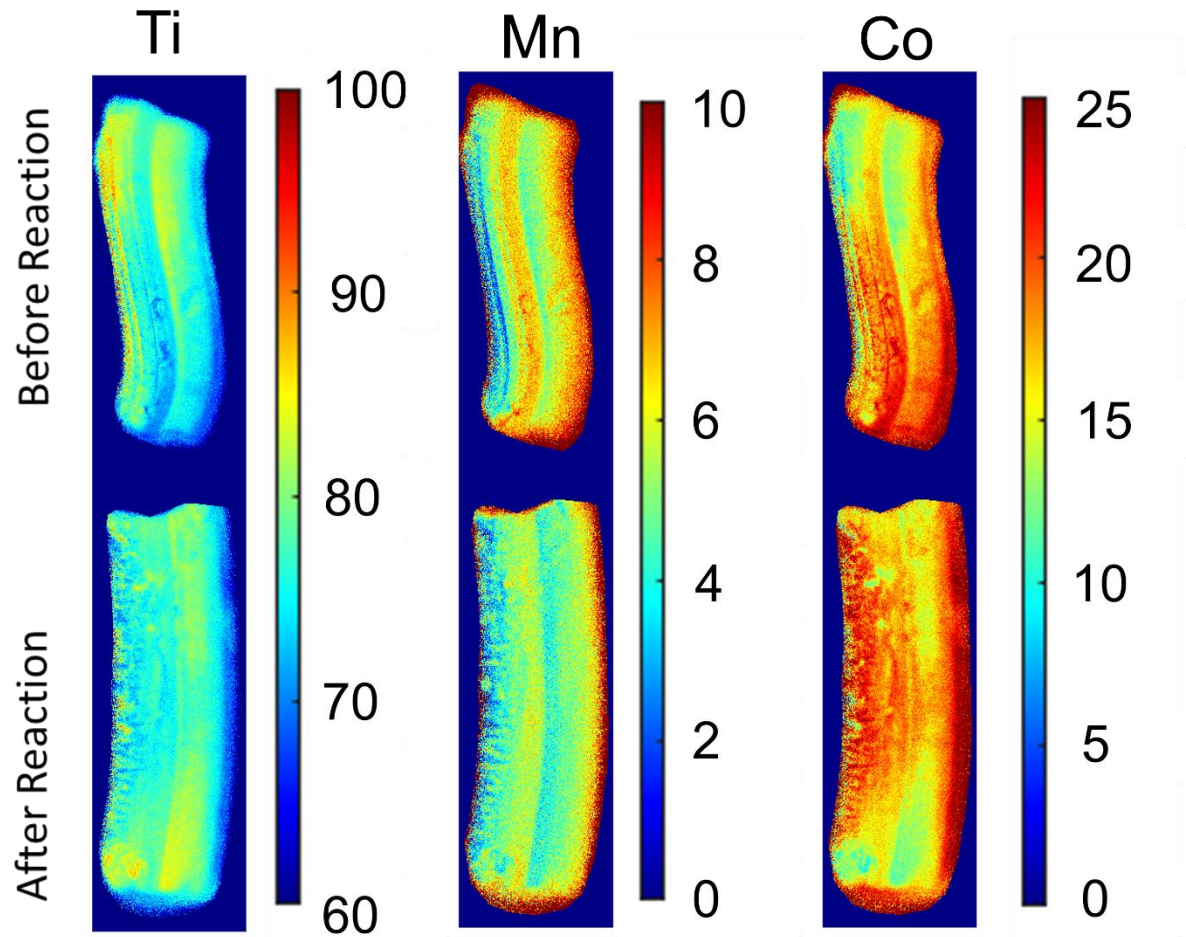


Figure S18 -  $\mu$ -XRF images (intensity (%)) of the lateral faces of the 3 wt. % Mn samples extracted before and after reaction for 300 h.

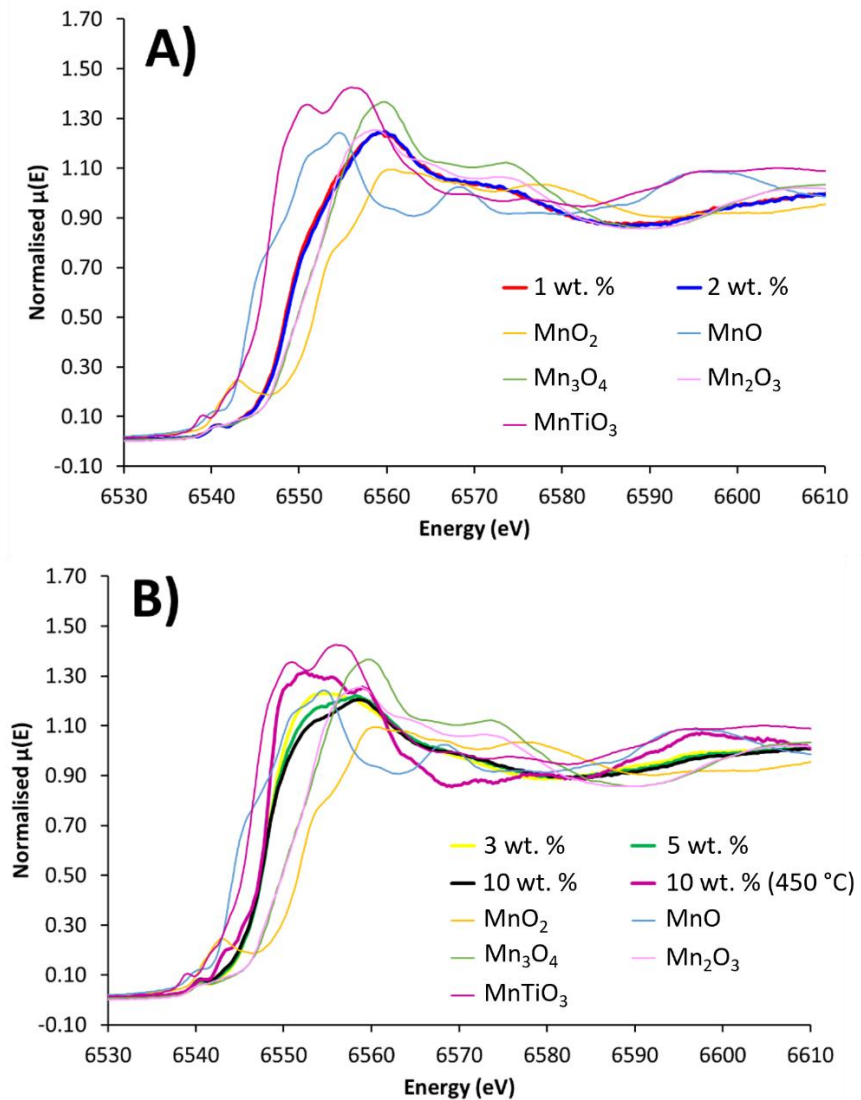


Figure S19 - Comparing Mn K-edge spectra of A) 1 and 2 wt. % CoMn/TiO<sub>2</sub> species and B) 3, 5, 10 and 10 wt. % Used CoMn/TiO<sub>2</sub> samples with a range of oxidic standards.